Published in final edited form as:
Cell Metab. 2014 July 1; 20(1): 73–84. doi:10.1016/j.cmet.2014.04.006.

BRD7 regulates XBP1s' activity and glucose homeostasis through its interaction with the regulatory subunits of PI3K

Sang Won Park[1,*], **Hilde Herrema**[1], **Mario Salazar**[1], **Isin Cakir**[1], **Serkan Cabi**[1], **Fatma Basibuyuk Sahin**[1], **Yu-Hsin Chiu**[2,3], **Lewis C. Cantley**[2,3,4], and **Umut Ozcan**[1,*]

[1]Division of Endocrinology, Boston Children's Hospital, Harvard Medical School, Boston MA 02115, USA

[2]Department of System Biology, Harvard Medical School, Boston, MA 02115, USA

[3]Division of Signal Transduction, Beth Israel Deaconess Medical Center, Boston, MA 02115, USA

[4]Department of Medicine, Weill Cornell Medical College, New York City, NY 10065, USA

Summary

Bromodomain-containing protein 7 (BRD7) is a member of the bromodomain-containing protein family that is known to play role as tumor suppressors. Here, we show that BRD7 is a component of the unfolded protein response (UPR) signaling through its ability to regulate X-box binding protein1 (XBP1) nuclear translocation. BRD7 interacts with the regulatory subunits of phosphatidyl-inositol3-kinase (PI3K) and increases the nuclear translocation of both p85α/β and XBP1s. Deficiency of BRD7 blocks the nuclear translocation of XBP1s. Furthermore, our *in vivo* studies have shown that BRD7 protein levels are reduced in the liver of obese mice, and reinstating BRD7 levels in the liver restores XBP1s nuclear translocation, improves glucose homeostasis, and ultimately reduces the blood glucose levels in the obese and diabetic mouse models.

Keywords

Bromodomain-containing protein 7 (BRD7); X-box binding protein1 (XBP1); Endoplasmic reticulum (ER) stress; Unfolded protein response (UPR); Diabetes

Introduction

Obesity is a fast growing global health problem and is the leading cause for development of type 2 diabetes, nonalcoholic steatohepatitis, and cardiovascular disease (Hevener and Febbraio, 2010; Kahn and Flier, 2000; Muoio and Newgard, 2006; Qatanani and Lazar,

[*]To whom correspondence should be address: sangwon.park@childrens.harvard.edu, (617-919-4596), umut.ozcan@childrens.harvard.edu (617-919-4684).

2007; Sun and Karin, 2012). Increased insulin resistance and perturbed glucose tolerance in obesity are the main underlying pathologies for development of type 2 diabetes (Guilherme et al., 2008; Kadowaki et al., 2003; Konner and Bruning, 2012). Majority of the patients diagnosed with type 2 diabetes are obese (de Luca and Olefsky, 2006; Kitamura and Accili, 2004). Despite enormous efforts, the molecular mechanisms of obesity-induced insulin resistance and glucose intolerance remain incompletely understood. Therefore, understanding the molecular links between obesity, insulin resistance and type 2 diabetes is of crucial importance for the development of new therapeutic strategies.

The endoplasmic reticulum (ER) is a cellular organelle in which secretory and membrane-bound proteins are folded into their three-dimensional structures and lipids and sterols are synthesized (Palade, 1956). Certain conditions, such as nutrient deprivation, increased protein trafficking, exposure to free fatty acids, accumulation of unfolded or misfolded proteins in the lumen of ER, and alterations in calcium homeostasis, interfere with proper function of the ER (Fonseca et al., 2011; Park et al., 2010b; Schroder and Kaufman, 2005; Walter and Ron, 2011). Perturbations in ER homeostasis can create a condition defined as ER stress (Park and Ozcan, 2013; Ron and Walter, 2007; Schroder and Kaufman, 2005; Walter and Ron, 2011). ER stress activates a cascade of complex signaling networks, collectively referred to as unfolded protein response (UPR) (Marciniak and Ron, 2006; Park and Ozcan, 2013; Schroder and Kaufman, 2005; Walter and Ron, 2011; Wang and Kaufman, 2012). The UPR is initiated by PKR-like endoplasmic reticulum kinase (PERK), inositol requiring enzyme -1 (IRE1), and activating transcription factor-6 (ATF6).

IRE1 has kinase and endoribonuclease activities. Upon activation, the endoribonuclease domain of IRE1 cleaves the mRNA of a transcription factor called X-box binding protein1 (XBP1) and removes a 26-bp of intron, resulting in a higher molecular weight protein called the spliced form of XBP1 (XBP1s) (Calfon et al., 2002; Lee et al., 2002; Yoshida et al., 2001). While the main function of XBP1s is to increase the folding capacity of the ER, it also regulates components in the ER-associated degradation (ERAD) pathway (Bernales et al., 2006; Lee et al., 2003; Merksamer and Papa, 2010; Ron and Walter, 2007; Zhang and Kaufman, 2008).

Over the last decade, we and others have shown that obesity leads to the development of ER stress in the liver, brain, and adipose tissues (Nakatani et al., 2005; Ozawa et al., 2005; Ozcan et al., 2009; Ozcan et al., 2004; Ozcan et al., 2008; Ozcan et al., 2006), which in turn contributes to the development of insulin resistance and type 2 diabetes. Previous observations have shown that genetic ablation of even one allele of XBP1 is sufficient to create insulin resistance and type 2 diabetes (Ozcan et al., 2004). We have recently demonstrated that reduced XBP1s activity in obesity plays a crucial role in the development of insulin resistance and type 2 diabetes (Lee et al., 2011; Park et al., 2010a; Zhou et al., 2011). Consistent with this notion, reinstating the activity of XBP1s in the liver of severely obese and diabetic mice reduced blood glucose levels to euglycemia and restored glucose homeostasis (Zhou et al., 2011).

We previously have reported that XBP1s interacts with the regulatory subunits of the class IA phosphotidyl-inositol3-kinase (PI3K), p85α and p85β, (Park et al., 2010a; Winnay et al.,

2010), which is one of the main nodules in insulin signaling. The interaction between p85s and XBP1s is a prerequisite for the nuclear translocation of XBP1s (Park et al., 2010a). More importantly, we showed that disruption of the interaction between p85s and XBP1s is a major cause for the development of insulin resistance in obesity (Park et al., 2010a).

Bromodomain-containing protein 7 (BRD7) is a subunit of the polybromo-associated BRG1-associated factor (PBAF) complex with a molecular weight of about 75 kDa (Kaeser et al., 2008). It plays a role in transcriptional regulation by binding to acetylated histone through its bromodomain (Peng et al., 2006). It was shown that the expression level of BRD7 is significantly decreased in nasopharyngeal carcinoma (NPC) biopsies (Zhou et al., 2004). Furthermore, BRD7 was reported to participate in tumor suppression, cell cycle, and cell growth (Kaeser et al., 2008; Peng et al., 2007; Zhou et al., 2004). Recent work suggested that BRD7 binds to BRCA-1 and p53, and acts as a tumor suppressor (Burrows et al., 2010; Drost et al., 2010; Harte et al., 2010; Mantovani et al., 2010).

Cantley and his co-workers recently showed that BRD7 binds to p85α and increases its nuclear translocation (Chiu *et al.* submitted). Considering the effect of p85s on XBP1s nuclear translocation (Park et al., 2010a), we investigated whether BRD7 plays a role on regulation of XBP1s, ER stress, and glucose metabolism.

Results

BRD7 interacts with p85α and increases its nuclear translocation

To confirm the interaction between BRD7 and the regulatory subunit of PI3K, p85α, (Chiu *et al.* submitted, 2013), we expressed mouse BRD7 and p85α by infecting the 293HEK cells with adenoviruses that express BRD7 (Ad-BRD7) and flag-tagged p85α-(Ad-p85α-flag). Subsequently, we immunoprecipitated p85α using an anti-flag antibody, blotted the precipitate with an antibody specific for BRD7 and documented that BRD7 exists in p85α immunoprecipitates (Figure 1A). This result indicates that BRD7 and p85α interact. We also performed reverse immunoprecipitation, in which BRD7 were pulled down and the existence of p85α in the precipitates was examined. Results from this experiment confirmed the interaction of these two proteins (Figure 1B). Next, we investigated whether BRD7 modulates the nuclear migration of p85α. We infected 293HEK cells with increasing doses of Ad-BRD7 while keeping the expression of p85α constant, and then analyzed p85α levels in the nuclear fractions. Increasing the expression level of BRD7 led to a higher translocation of p85α to the nucleus (Figure 1C). We also tested whether BRD7 can increase the nuclear translocation of p85β by infecting 293HEK cells with increasing doses of Ad-BRD7 while keeping the expression of p85β constant. BRD7 led to increased nuclear translocation of p85β as well (Figure S1A).

These observations prompted us to investigate whether BRD7 has any effect on XBP1s, because we have previously shown that p85α/β binds to XBP1s and increases its nuclear translocation (Park et al., 2010a). For this purpose, we infected 293HEK cells with XBP1s-expressing adenovirus (Ad-XBP1s) at a constant dose along with incremental doses of Ad-BRD7. Indeed, we found that upregulating BRD7 level increases the nuclear translocation of XBP1s (Figure 1D) without increasing XBP1 mRNA levels (data not shown).

The next question we asked was how BRD7 increases the XBP1s nuclear translocation. We explored whether it is mediated through a direct interaction of BRD7 with XBP1s that is independent of p85α, or through the ability of BRD7 to regulate p85α and consequent XBP1s interaction. We first expressed BRD7 and XBP1s in 293HEK cells by infecting the cells with Ad-BRD7 and Ad-XBP1s and performed XBP1 immunoprecipitation. We blotted the precipitate with an antibody that is specific for BRD7 and showed that BRD7 and XBP1s can be co-immunoprecipitated (Figure 1E) indicating that these two proteins either directly interact or exist in the same protein complex. Considering the fact that both BRD7 and p85α can be immunoprecipitated with XBP1s (Park et al., 2010a), we asked whether BRD7 could directly bind to XBP1s in the absence of p85α/β . Thus, we knocked down p85α and p85β in mouse embryonic fibroblasts (MEFs) with an shRNA lentivirus system specific for p85α and p85β to create $p85\alpha^{-/-}\beta^{-/-}$ double knock down (DKD) cell line. We also created a control cell line, PLKO, using an empty lentivirus (PLKO) (Figure 1F). The interaction between BRD7 and XBP1s was observed in control PLKO cells (Figure 1F). However, this interaction was reduced in p85α/β-depleted DKD cells (Figure 1F). After obtaining these results, we investigated the nature of the interaction between BRD7 and XBP1s in p85α/β double knockout (DKO) cells. Following expression of BRD7 and XBP1s in p85α/β DKO cells, we performed XBP1s immunoprecipitation and investigated the presence of BRD7 in these precipitates. The interaction between BRD7 and XBP1s was not detected at all in p85α/β DKO cells (Figure 1G), indicating that p85α or p85β are necessary for BRD7-XBP1s interaction.

Since our results have shown that BRD7 interacts with XBP1s only in the presence of p85α/β, we then asked whether BRD7 is still capable of increasing the nuclear translocation of XBP1s at the absence of p85α/β. For this purpose, we infected the DKD, DKO, and their control cells with Ad-XBP1s at a constant dose and increasing doses of Ad-BRD7. We found that BRD7 could not increase transport of XBP1s to the nucleus in DKD cells as it did in PLKO cells (Figure 1H). Moreover, XBP1s were not detected in the nucleus of DKO cells even with overexpression of BRD7 (Figure 1I), indicating that the presence of p85α/β is required for BRD7 to force XBP1s to the nucleus.

BRD7 and p85α are required for the activity of XBP1s

The above findings indicate that BRD7 plays a role in XBP1s' nuclear migration. To further investigate the nature of the interaction between p85α, XBP1s, and BRD7, we expressed p85α and XBP1s in the cells either with or without BRD7 (Figure 2A). Subsequently, we isolated the cytoplasmic and nuclear fractions and performed XBP1s immunoprecipitation from both compartments. BRD7 expression reduced the amount of p85α-XBP1s complex in the cytoplasm (Figure 2A left panel). However, it increased the nuclear amount of p85α-XBP1s complex (Figure 2A right panel). These results indicate that BRD7 enhances the binding of p85 to XBP1s and increases its nuclear translocation.

We previously have shown that p85α and p85β form a heterodimer, which can be disrupted by insulin treatment (Park et al., 2010a). We have reported that insulin promotes the nuclear translocation of XBP1s by increasing the binding of p85α/β monomers to XBP1s (Park et al., 2010a). Considering this data, we investigated whether insulin regulates BRD7-p85-

XBP1s complex. First, we expressed p85α and BRD7 in 293HEK cells by infecting with Ad-BRD7 and Ad-p85α-flag. Following serum starvation, we stimulated the cells with insulin (500 nM) for various time points. Subsequently, we immunoprecipitated p85α with an anti-flag antibody and immunoblotted for BRD7 to investigate whether the interaction between p85α and BRD7 is affected by insulin treatment. The results showed that insulin enhances the association of p85α and BRD7 in the nuclear fractions (Figure 2B). We then investigated the effect of insulin on the formation of BRD7-p85α-XBP1s complex. We infected 293HEK cells with Ad-BRD7 and Ad-XBP1s-flag and following an overnight serum deprivation, we stimulated the cells with insulin (500 nM) for 0.5 and 2 hours. XBP1 was then immunoprecipitated and the immunoprecipitates were blotted for BRD7. Insulin led to increased binding of BRD7 to XBP1s in the nucleus (Figure 2C).

To further understand how BRD7 is regulated, we infected 293HEK cells with increasing doses of Ad-BRD7 and a constant dose of Ad-p85α-flag and Ad-p85β-myc, and then immunoprecipitated p85α using an anti-flag antibody, followed by western blot using anti-myc antibody to analyze whether the association between p85α and p85β is affected by BRD7 expression. This results showed that increasing BRD7 expression disrupts the p85α/β heterodimer (Figure 2D).

We next examined whether BRD7 ability to increase nuclear translocation of XBP1s also has positive modulatory effects on XBP1s activity. For this purpose, we expressed BRD7 in MEFs and analyzed the mRNA levels of various genes that are the targets of XBP1s, such as endoplasmic reticulum-localized DnaJ homologues (*Erdj4*), homocysteine-inducible, endoplasmic reticulum stress-inducible, ubiquitin-like domain member 1 (*Herpud1*; *Herp*), and endoplasmic reticulum oxidoreductin 1α (*Ero1α*). Quantitative PCR (qPCR) analysis showed that expression of BRD7 significantly upregulated the transcription of *Erdj4*, *Herp*, and *Ero1α* (Figure 2E), suggesting that BRD7 increases the activity of XBP1s as a transcription factor in the nucleus.

In order to address whether BRD7 is required in the nuclear translocation process of XBP1s, we first identified an shRNA sequence that is specific for BRD7 mRNA, showed the efficacy of this shRNA and then cloned this sequence into an adenovirus vector (Ad-BRD7shRNA). Infections of MEFs led to a highly significant reduction in BRD7 mRNA levels (Figure S2A and S2B). Subsequently, we investigated the nuclear migration pattern of XBP1s in the absence of BRD7. For this purpose, we expressed BRD7shRNA along with XBP1s in 293HEK cells. There was a major reduction in the nuclear XBP1s levels in BRD7-depleted cells when compared to the control cells or cells overexpressing BRD7 (Figure 2F). To further confirm this result in *in vivo*, we injected eight-week-old male lean mice with 1.5×10^8 plaque-forming unit (pfu)/g of Ad-BRD7shRNA or Ad-LacZshRNA via the tail vein. We previously reported that fasting wild-type mice for 24 hours and refeeding food *ad libitum* for one hour markedly increases the XBP1 splicing and nuclear translocation of XBP1s (Park et al., 2010a). This increased nuclear translocation of XBP1s with refeeding was also observed in the mice that were injected with Ad-LacZshRNA, but to a comparably lesser extent in the mice that were injected with Ad-BRD7-shRNA (Figure 2G), without any change in the splicing of XBP1 mRNA (Figure 2H). This suggests that reduced nuclear XBP1s levels in the liver of Ad-BRD7shRNA injected mice are not due to a defect in XBP1

splicing. In parallel to these results, expression of XBP1 target genes were reduced and expression of CHOP was increased in the liver of Ad-BRD7-shRNA-injected group when compared to those that were injected with Ad-LacZ-shRNA (Figure 2I).

BRD7 overexpression in the liver of the *ob/ob* mice establishes euglycemia

Considering the defect in hepatic XBP1s nuclear translocation in obese mice and also our *in vitro* results that show BRD7 is involved in the regulation of XBP1s nuclear migration and activity, we investigated whether BRD7 levels are reduced in the liver of obese mice. Indeed, we found that there was a significant reduction in the BRD7 protein levels in the liver of *ob/ob* mice when compared with the lean controls (Figure 3A). Furthermore, we showed that BRD7 mRNA levels were increased during refeeding period in wild-type mice, but this increment was lost in *ob/ob* mice (Figure 3B).

Obesity is a condition of hyperinsulinemia and elevated ER stress. Therefore, we sought to investigate whether prolonged insulin stimulation or ER stress is a cause for the reduced BRD7 expression level in obesity. For this purpose, we first induced ER stress in MEFs by treating the cells with tunicamycin at various doses (0.1 to 10 μg/ml) for one hour following overnight starvation and analyzed the endogenous BRD7 protein and mRNA levels by performing western blot and qPCR, respectively. The results showed no significant difference in BRD7 expression levels after tunicamycin treatment (Figure S3A and S3B). In addition, we treated MEFs and Fao cells with tunicamycin at the concentration of 3 μg/ml for one, two, and three hours. The treatment of the cells with tunicamycin did not alter BRD7 expression patterns either (Figure S3C-S3F). Next, after overnight starvation, we stimulated Fao and 293HEK cells with insulin (500 nM) for different time points. Exposure of the cells to insulin did not affect BRD7 gene expression levels (Figure S3G-S3I).

We previously have reported that overexpression p85α or p85β in the liver of obese and diabetic mice reinstates the nuclear translocation of XBP1s, reduces ER stress, improves glucose tolerance and ultimately reduces the blood glucose levels (Park et al., 2010a). Given that BRD7 has ability to increase the nuclear translocation of both p85α/β and XBP1s, and that its expression is significantly reduced in the liver of obese mice, we hypothesized that up-regulating the expression of BRD7 in the liver of obese and diabetic mice would improve glucose tolerance and reduce blood glucose levels. To test this hypothesis, we overexpressed BRD7 in the liver of *ob/ob* mice by tail vein injection of Ad-BRD7 and Ad-LacZ as a control at a dose of 1×10^8 pfu/g (Figure S3J and S3K). After three days of injection, we fasted the mice for six hours and measured the basal blood glucose levels. Ad-BRD7-injected group had significantly lower blood glucose levels than those in the Ad-LacZ injected group (Figure 3C). There were no difference in the body weight or the food intake between Ad-BRD7 and Ad-LacZ injected groups (Figure S3L and S3M). Glucose tolerance test (GTT) was performed at day five post-injection and the result revealed a major improvement in the glucose disposal rate in the Ad-BRD7 injected group (Figure 3D). Insulin tolerance test (ITT) at day seven showed that whole body insulin sensitivity was improved (Figure 3E).

Next, we investigated whether hepatic insulin receptor signaling is altered after BRD7 expression in the *ob*/*ob* mice. To do this, we infused either insulin (0.35 IU/kg) or saline

through the portal vein into the liver of *ob*/*ob* mice on post-injection day eight. The phospho/total insulin receptor (IR) and insulin receptor substrate 1 (IRS1) values were slightly increased but did not reach to significant levels in Ad-BRD7-injected group. (Figure 3F). However, Akt^{Thr308} and Akt^{Ser473} phosphorylations were significantly increased (Figure 3F), These results indicate that BRD7 expression in the liver leads to an increase in the sensitivity of IRS1–Akt axes of IR signaling cascade.

Furthermore to investigate whether BRD7 overexpression increases the association of p85 with IRS proteins, we performed p85 immunoprecipitation from the liver tissues that were infused with insulin or saline, then immunoblotted for IRS1 and IRS2. The results showed that the interaction between p85s and IRSs are indeed increased after insulin stimulation in Ad-BRD7-injected group (Figure 3G) when compared to those of Ad-LacZ-injected group.

Next, we sought to investigate whether an increase in BRD7 expression leads to increased XBP1s nuclear translocation and a corresponding up-regulation of XBP1s target genes in *in vivo* settings. For this purpose, we injected eight-week-old male *ob*/*ob* mice with Ad-BRD7 and Ad-LacZ at a dose of 1×10^8 pfu/g through the tail vein. The overexpression of Ad-BRD7 in the liver of *ob*/*ob* mice greatly increased XBP1s nuclear translocation (∼12 fold upregulation; Figure 4A). In line with the increased nuclear translocation of XBP1s, target gene expression, such as *Erdj4*, *Herp*, and *Ero1α*, were significantly upregulated at both mRNA and protein levels (Figure 4B and 4C).

In parallel, we observed decreased PERK phosphorylation in Ad-BRD7 injected *ob*/*ob* mice's liver when compared to those in Ad-LacZ injected group (Figure 4D and S4A). Accordingly, the levels of phospho-eIF2α^{Ser51}, a direct downstream target of phospho-PERK, were also decreased (Figure 4D and S4B). These results indicate that ER stress is reduced after BRD7 overexpression in the liver of *ob/ob* mice. Considering our previously published results showing that XBP1s leads to FoxO1 degradation (Zhou et al., 2011), we investigated the nuclear and total levels of FoxO1. BRD7 overexpression led to a major decrease in both nuclear and total FoxO1 levels in the liver of *ob/ob* mice. (Figure 4E). Accordingly, gene expressions of glucose-6-phosphatase (*G6P*), fructose bisphosphatase (*FbP*), and phosphoenolpyruvate carboxykinase (*Pepck*) were significantly reduced in BRD7-overexpressing mice's livers (Figure 4F). Furthermore, even macroscopically, BRD7-overexpressing livers had a healthier appearance than the Ad-LacZ-injected control groups (Figure 4G). H&E staining of the sections from the liver of Ad-LacZ- and Ad-BRD7-injected *ob*/*ob* mice showed a major decrease in the lipid droplets (Figure 4H). In line with these observations, analysis of liver triglyceride (TG; mg/dl) content showed a significant reduction in the liver of Ad-BRD7-injected *ob*/*ob* mice (Figure 4I). Analysis of lipogenic gene expression such as acetyl co-A carboxylase 1 (*Acc1*,), fatty acid synthase (*FasN*), and diacylglycerol acyltransferase 2 (*Dgat2*) were significantly reduced in BRD7-overexpressing mice's livers (Figure 4J). Taken together, these results indicate that BRD7 also have anti-lipogenic properties.

Restoration of BRD7 in the liver of DIO mice improves glucose metabolism

Our data thus far showed that BRD7 protein levels are reduced in genetically obese and diabetic *ob*/*ob* mice and that restoration of BRD7 levels re-establishes glucose homeostasis.

Next, we sought to examine the BRD7 expression levels in diet-induced obese (DIO) mouse model. For this purpose, wild-type lean C57BL/6 male mice were placed either on high fat (HFD, 45 kcal% from fat) or normal chow diet (NCD) feeding soon after weaning at the age of 3.5 weeks and maintained on the same diet for 16 weeks. At the end of 16-week feeding period, we examined the protein levels of BRD7 in the liver of HFD- and NCD-fed groups. We observed a marked reduction in the hepatic level of BRD7 in the HFD-fed mice (Figure 5A). We then compared the BRD7 protein levels amongst wild-type mice on NCD, genetically obese *ob*/*ob* mice, and wild-type mice that were kept on HFD for eight weeks. The expression levels of BRD7 in the liver of eight-week HFD-fed mice were also significantly reduced, and this reduction was comparable to that seen in *ob*/*ob* mice (Figure 5B). Next, we overexpressed BRD7 or LacZ (as a control) in the liver of mice that were fed either NCD or HFD for eight weeks by tail vein injection of the corresponding adenoviruses at a dose of 5×10^7 pfu/g. After three days of injection, we measured the blood glucose levels and showed that the blood glucose levels of the Ad-BRD7 injected group were significantly lower compared to those of the Ad-LacZ injected group (Figure 5C). GTT was performed at day five post-injection and the result revealed a significant improvement in the glucose disposal rate in the Ad-BRD7 injected group (Figure 5D). In addition, the overexpression of BRD7 in the liver of HFD mice group restored the ability of XBP1s to translocate to the nucleus while Ad-LacZ injected mice group could not translocate XBP1s to the nucleus (Figure 5E). Next, we fasted these two groups for 24 hours and then gave them food *ad libitum* for one hour. We collected the liver and determined gene expression profiles of XBP1s target genes. Refeeding led to significantly higher mRNA levels of *Erdj4*, *Herp*, and *Ero1*α in the Ad-BRD7-injected group compared to the Ad-LacZ group (Figure 5F-H), indicating that BRD7, as seen in genetically obese models, also increases XBP1s activity in the HFD-fed obese mice.

Discussion

Over the last decade, XBP1s has been emerged as a central player in maintenance of glucose homeostasis due to its ability to reduce ER stress, increase insulin sensitivity, and also degrade FoxO1 through a direct protein interaction (Lee et al., 2011; Ozcan et al., 2004; Park et al., 2010a; Zhou et al., 2011). Reduced XBP1s activity in obesity due to impaired nuclear translocation is a major cause for the development of ER stress and consequently insulin resistance and type 2 diabetes. Re-instating the activity of XBP1s in obese and diabetic mice through genetic manipulations greatly improves glucose homeostasis (Zhou et al., 2011). Therefore, it is important to understand the mechanisms leading to the reduced XBP1s activity in obesity to create potential targets for the treatment of type 2 diabetes.

Findings presented in this work, for the first time, show a role for BRD7 in metabolic homeostasis and also in UPR signaling. We previously have reported that p85α and p85β form heterodimers, which can be disrupted by insulin (Park et al., 2010a). Free monomeric p85 interacts with XBP1s and imports XBP1s to the nucleus. In this report, we added another crucial component to this mechanism. We document that BRD7 interacts with p85α/β and that insulin enhances the interaction between BRD7 and p85. Consequently, insulin increases the formation of BRD7-p85-XBP1s complex, which in turn leads to increased nuclear translocation and activity of XBP1s. However, further detailed

investigation is needed to understand the exact molecular mechanism by which insulin modulates BRD7-p85 complexes to regulate the nuclear translocation of XBP1s.

Here, we document that decreased BRD7 levels in obesity is a critical pathology for reduced XBP1s activity and consequently for the development of ER stress, glucose intolerance, and type 2 diabetes. Our observations indicate that increasing BRD7 levels in the liver of obese and diabetic mice reinstates XBP1s nuclear translocation, reduces ER stress, and significantly improves glucose homeostasis. Furthermore, our results are the first to document the requirement for BRD7 in XBP1s' action, which is one of the master regulators of UPR signaling. This indicates that BRD7 is also an important element in UPR signaling. In the mean time, BRD7 has been shown to interact with p53 and plays a role as a tumor suppressor. It is possible that it might have other functions inside the cells. Therefore, we can not completely rule out the possibility that the improvement in glucose homeostasis could also have been affected by other effects of BRD7 in addition to its regulatory effects on XBP1s. Future studies are required to answer this question and to understand the detailed role of BRD7 in UPR signaling and diseases, pathology of which is contributed by UPR.

It is interesting to note that installment of BRD7 levels in the liver of obese and diabetic mice, while increasing the insulin-stimulated Akt activation (IRS1→PI3K→Akt axis), it does not increase the sensitivity of IR→IRS1 axis. Our previous observations have shown that XBP1s reduces glucose intolerance and establishes metabolic homeostasis through both insulin-dependent and -independent mechanisms (Zhou et al., 2011). High levels XBP1s expression enhances insulin receptor signaling in the liver. However, in the mean time, hepatic overexpression of XBP1s in the liver-specific IRS1 and IRS2 double knockout mice can also improve glucose homeostasis through increasing FoxO1 degradation, without changing its mRNA levels (Zhou et al., 2011). Gain of function studies for BRD7 in the liver increased XBP1s nuclear translocation and led to highly significant reductions in FoxO1 protein levels, without decreasing its mRNA levels. These results together with increased Akt activation would explain how BRD7 improved glucose tolerance in obese and diabetic mice.

However, how BRD7 expression increases the sensitivity of IRS1→PI3K→Akt axis without an increase in the sensitivity of IR→IRS1 axis remains unclear and future experiments are needed for further understanding of BRD7 effect on Akt activation. One possible explanation could be that BRD7, by increasing the availability of either p85s (p85a α or p85β) to XBP1s, making the other isoform more available to p110, and increasing the interaction of p85/p110 complex with IRS1. In addition, the liver has p85α/β in excess over the p110 catalytic subunits (Brachmann et al., 2005; Ueki et al., 2002; Ueki et al., 2003). It was reported that the p85 monomers competes with p85-p110 heterodimers for binding to IRS proteins and suppress PI3K signaling (Luo et al., 2005). Therefore, importing p85α/β into the nucleus with BRD7 overexpression may enhance Akt signaling by reducing the sequestration of IRS1 by monomeric p85.

In addition, p85s and its other isoforms might have different functions in different tissues or cell lines depending on the ratio of the different subunits. As recently reported, down regulation of p85 in Akita diabetic mice delays the onset and severity of complications, this

has been suggested to be due to a reduction in ER stress-induced apoptosis (Winnay et al., 2014).

Insulin is a crucial hormone for life. Insulin resistance in obesity, despite leading to the development of type 2 diabetes, could have evolved to protect organism from possible detrimental site effects of prolonged exposure to high levels of circulating insulin (Accili and Arden, 2004; Kenyon, 2010; Russell and Kahn, 2007). Indeed, several insulin resistance models, such as adipocyte specific insulin receptor (Bluher et al., 2003) or brain specific IRS2 knock out mice have extended life spans (Taguchi et al., 2007). One of the main side effects of insulin action is upregulating the lipogenesis in various tissues. In this sense BRD7-mediated regulation of glucose homeostasis could be a new and exciting therapeutic target, through which glucose homeostasis can be established without increasing lipogenesis both in the liver and also adipose tissues. Our results indicate that BRD7 expression in the liver of obese mice significantly reduces hepatosteatosis, which is one of the leading causes for the development of cirrhosis in obese population. Furthermore, obesity is related to increased risk of various cancers and increased insulin action could be contributing to the development of cancers in obesity. Considering the anti-tumorigenic effect of BRD7, activators of this molecule might be effective in reducing the cancer risk, while re-establishing the metabolic homeostasis.

In summary, our current work introduces a protein with anti-diabetic effects, which holds a potential to be targeted for the treatment of type 2 diabetes in obesity.

Experimental Procedures

Cell culture—Mouse Embryonic Fibroblast (MEF), 293A, 293T, and 293HEK cells were maintained in DMEM with 10% FBS, 10 U/ml penicillin, and 1 μg/ml streptomycin. Fao cells were maintained in RPMI with 10% FBS, 10 U/ml penicillin, and 1 μg/ml streptomycin. Cells were split at a density of 3.5×10^5 in 10 cm dish or 2×10^5 in 6 cm dish 16 hours prior to the experiments. Cells were maintained at 37°C in a 5% CO_2 humidified atmosphere.

Western blotting—For total cell lysates, cells were lysed in lysis buffer which contained 25 mM Tris (pH 7.4), 2 mM $NaVo_4$, 10 mM NaF, 10 mM $Na_4P_2O_7$, 1 mM EGTA, 1 mM EDTA, and 1% NP-40. Protease inhibitor cocktail and PhosSTOP were added fresh to the lysis buffer before each experiment. Equivalent concentration of protein (ranging 1–3 μg/μl) from each sample was placed in 1.5 ml tubes. Protein was denatured in 1×Laemmlie buffer by boiling at 100°C for five minutes, except the samples for BRD7 analysis from tissues; these samples were not boiled after adding laemmlie buffer. The tubes were kept at room temperature for 15 minutes before loading to SDS-PAGE gel. After resolving in SDS-PAGE, the proteins were transferred onto polyvinylidene fluoride (PVDF) membrane. The membrane was blocked in Tris-Buffered Saline (TBS, pH 7.4) with 10% blocking reagent provided with BM Chemiluminescence blotting substrate (POD) assay system for one hour, followed by incubation with primary antibody in Tris-Buffered Saline-Tween (TBST, pH 7.4) with 5% blocking reagent for overnight at 4°C. After the incubation, the membrane was washed three times in TBST, followed by incubation with secondary antibody in TBST-10%

blocking reagent for one hour and washed again in TBST (three times for 20 min). Immunoblots were developed using a chemiluminescence assay system, and bands were visualized using Kodak exposure films. For stripping, the membranes were vigorously shook in stripping buffer (2% SDS, 100 mM 2-mercaptoethanol in TBS) at 50°C for 20 minutes followed by three washes with TBST. Densitometry was performed with Image J (NIH) for quantifications.

Nuclear protein extraction—For nuclear protein extraction from cells in 6 cm plate, cells were removed from dishes by scraping with 300 μl of cytoplasmic lysis buffer (10 mM Hepes (pH 7.5), 2 mM $MgCl_2$, 1 mM EDTA, 1 mM EGTA, 10 mM KCl, 10 mM NaF, 0.1 mM Na_3VO_4, Protease inhibitor cocktail, and PhosSTOP). Following 15 minutes of incubation on ice, 25 μl of 10% NP-40 were added and vortexed for 10 seconds. The cells were centrifuged for one minute at 16,000 xg, and supernatants were collected to obtain the cytoplasmic fractions. The pellets were resuspended in 200 μl of nuclear lysis buffer (25 mM Hepes (pH 7.5), 500 mM NaCl, 10 mM NaF, 10% Glycerol, 0.2% NP-40, 5 mM $MgCl_2$, and 10 mM DTT). RIPA buffer was used instead of nuclear lysis buffer for immunoprecipitation experiments. The suspension was incubated on ice for 30 minutes. During this incubation, lysates were vortexed every 10 minutes. Finally, cells were centrifuged for 10 minutes at 16,000 xg to obtain nuclear proteins. For nuclear extraction from liver tissues, 50 mg of liver tissue were cut in small pieces and washed once with ice-cold PBS. Nuclear proteins were isolated using a commercially available kit from Pierce according to the manufacturer's instructions with no modifications.

Immunoprecipitation—Lysates in RIPA buffer were incubated with antibody (0.3–0.6 μg) overnight at 4 °C with gentle rotation. 80 μl of pro tein A-Sepharose CL-4B beads (for rabbit IgG) or protein G-Sepharose CL-4B beads (for mouse IgG) were added to the tubes and rotated at 4 °C for two hours. Beads were precipitated by centrifugation at 16,000 xg for 30 seconds and washed them three times with cold RIPA buffer containing 150 mM NaCl. The pellet were resuspended in 2x Laemmlie buffer and incubated at 100°C for 5 minutes. The supernatants were used for western blot.

Lysis of liver tissue—For direct immunoblotting, 50 mg of liver tissue was homogenized with Tissue Lyser II (Qiagen) in 1 ml of ice-cold tissue lysis buffer (25 mM Tris-HCl (pH 7.4), 10 mM Na_3VO_4, 100 mM NaF, 50 mM $Na_4P_2O_7$, 10 mM EGTA, 10 mM EDTA, 1% NP-40, 2 mM PMSF, Protease inhibitor cocktail, and PhosSTOP). Homogenized tissue was incubated at 4 °C for one hour and centrifuged a t 16,000 xg for 30 minutes. The lipid layer was carefully removed using cotton swab, and the supernatant was centrifuged again for one hour at 16,000 xg and 4 °C before coll ecting proteins for western blot.

XBP1 splicing assay—The splicing of XBP1 from cDNA was analyzed by performing PCR using Taq DNA polymerase. The PCR conditions were as follows: 94°C for 3 minutes; 29 cycles of 94°C for 30 seconds, 58°C for 30 seconds, and 72°C for 30 seconds; and 72°C for 3 minutes. The primer sequenc es are as follow:

Forward: 5′ACA CGC TTG GGA ATG GAC AC3′

Reverse: 5′CCA TGG GAA GAT GTT CTG GG3′

Production and transduction of shRNA lentivirus—293T cells were split in 10 cm dish and transfected with pLKO, pLP1, pLP2, and pVSV-G using Lipofectamine according to manufacturer's instruction. The shRNA sequences carried in pLKO vector for p85α and p85β were as follows:

p85α:
5′CCGGCAACCGAAACAAAGCGGAGAACTCGAGTTCTCCGCTTTGTTTCGGTTGTTTTTG3′

p85β:
5′CCGGCCTGTGTCCAAGTACCAACAACTCGAGTTGTTGGTACTTGGACACAGGTTTTT3′

Media was replaced with fresh media 16 hours after the transfection. Cells were incubated at 37°C in a 5% CO_2 humidified atmosphere for 48 hours. The viral particles were harvested by passing the supernatant through a 0.45 μm filter. Viruses were concentrated by ultracentrifugating for 1.5 hours at a speed of 50,000 xg. The viral pellet was resuspended in a small volume of medium and left at 4 °C for overnight. To transduce cells with viruses, viral supernatants were added to the cells in the presence of polybrene at a final concentration of 2 μg/ml.

Production of adenoviral vectors—Mouse BRD7 was obtained from performing PCR with cDNA synthesized from MEFs using following primer pairs.

Forward: 5′ATG GGC AAG AAG CAC AAG AA3′

Reverse: 5′TCA GCT CGC GTC AGG CCC AC3′

PCR was performed with the following conditions: 94°C for 10 minutes; 18 cycles of 94°C for 30 seconds, 65°C for 30 seconds, and 72°C for 6 minute; and 72°C for 15 minutes. After PCR, products were cleaned with PCR purification kit and cloned into pENTR3C vector to create pENTR3C-mBRD7, which was recombined to pAd to create adenoviral vector pAd-BRD7. The shRNA sequences for BRD7shRNA were as follows:
5′CCGGGCCAAGATTACCCGTATGTTACTCGAGTAACATACGGGTAATCTTGGCTTTTT3′

Adenovirus production—Adenovirus vector that contain a gene of p85α, p85β, BRD7, XBP1s, and BRD7shRNA were constructed using gateway recombination system from Invitrogen. Adenovirus vectors were digested with *PacI* and used to transfect the 293A producer cell line in a 6-well-plate. The media were replaced with DMEM containing 10% FBS and 1% penicillin/streptomycin the next day, and the cells were transferred to 10 cm tissue culture dishes 24 hours after the transfection. The culture media were replaced with fresh media every 2–3 days until cytopathic effect (CPE) was observed. Cells were harvested when 80% CPE were observed, and the freezing and thawing cycles at −80°C and 37°C were repeated four times. The cell lysate was centrifuged at 1,200 xg for 30 minutes at room temperature, and the supernatants containing the adenovirus particles were stored at −80°C.

Adenovirus transduction—To infect cells with adenoviruses, cells in 6 cm plates were washed with culture medium containing 1% FBS and incubated with 2.5 ml of media containing 1% FBS and adenoviruses. Cells were carefully rotated every 15 minutes for one hour, and incubated for 16 hours after adding 1.5 ml of media containing 1% FBS.

Glucose tolerance test (GTT)—Mice were fasted overnight (6 pm–9 am) and D-glucose (2 g/kg for lean wild-type mice; 0.5 g/kg for *ob*/*ob*; and 1 g/kg for DIO mice) was administrated intraperitoneally. Blood glucose levels were measured from the tail before glucose administration and at 15, 30, 60, 90, 120 minutes following glucose administration.

Insulin tolerance test (ITT)—Mice were fasted for six hours (8 am–2 pm) and recombinant human insulin from Eli Lilly was administrated intraperitoneally (1 IU/kg for lean wild-type mice and 1.5 IU/kg for *ob*/*ob* and DIO mice). Blood glucose levels were measured from the tail before glucose administration and at 15, 30, 60, 90, 120 minutes following insulin administration.

Adenovirus injection—Adenovirus was thawed at room temperature immediately before injection and diluted with saline to a final volume of 100 μl per mouse. Mice were restrained in a restrainer and the tail was mildly heated with a heating lamp to achieve vasodilatation. Adenovirus was injected through the tail vein slowly with a 30-gauge needle. After injection, mild pressure was applied at the spot of injection until no bleeding was achieved to prevent the backflow of viral solution.

Analysis of *in vivo* insulin receptor signaling—Mice for fasted for six hours (8 am – 2 pm) and anesthetized with xylazine-ketamine. Insulin (0.35 IU/kg) or saline was infused into the liver of mice through the portal vein. Four minutes after infusion, the liver was extracted, flash frozen in liquid nitrogen, and stored in −80°C until processing.

Animal experiments—All the performed animal experiments were approved by Boston Children Hospital, IACUC.

Statistical analyses—Error bars represent the SEM. Statistical significance was determined by Student's t test or multifactor ANOVA with the factor of time. When ANOVA indicated a significant difference between the groups, we compared the groups using a stricter criterion for statistical significance according to the Bonferroni rule as follows: corrected P value = pairwise P value × number of comparisons. Significance was accepted at $*P < 0.05$, $**P < 0.01$, $***P < 0.001$.

Supplementary Material

Refer to Web version on PubMed Central for supplementary material.

Acknowledgments

We thank Dr. Morris F. White (Boston Children's Hospital, Harvard Medical School) for providing us with anti-IRS1 and IRS2 antibodies. This work was supported by National Institutes of Health R01 grant (R01DK081009) provided to U.O., the Timothy Murphy funds provided to the Division of Endocrinology, Boston Children's

Hospital, and National Institutes of Health K99 grant (K99DK093788) provided to S.W.P. U.O is a scientific founder, SAB member, and share holder of ERX Pharmaceuticals.

References

Accili D, Arden KC. FoxOs at the crossroads of cellular metabolism, differentiation, and transformation. Cell. 2004; 117:421–426. [PubMed: 15137936]

Bernales S, Papa FR, Walter P. Intracellular signaling by the unfolded protein response. Annu Rev Cell Dev Biol. 2006; 22:487–508. [PubMed: 16822172]

Bluher M, Kahn BB, Kahn CR. Extended longevity in mice lacking the insulin receptor in adipose tissue. Science. 2003; 299:572–574. [PubMed: 12543978]

Brachmann SM, Ueki K, Engelman JA, Kahn RC, Cantley LC. Phosphoinositide 3-kinase catalytic subunit deletion and regulatory subunit deletion have opposite effects on insulin sensitivity in mice. Mol Cell Biol. 2005; 25:1596–1607. [PubMed: 15713620]

Burrows AE, Smogorzewska A, Elledge SJ. Polybromo-associated BRG1-associated factor components BRD7 and BAF180 are critical regulators of p53 required for induction of replicative senescence. Proc Natl Acad Sci U S A. 2010; 107:14280–14285. [PubMed: 20660729]

Calfon M, Zeng H, Urano F, Till JH, Hubbard SR, Harding HP, Clark SG, Ron D. IRE1 couples endoplasmic reticulum load to secretory capacity by processing the XBP-1 mRNA. Nature. 2002; 415:92–96. [PubMed: 11780124]

de Luca C, Olefsky JM. Stressed out about obesity and insulin resistance. Nat Med. 2006; 12:41–42. discussion 42. [PubMed: 16397561]

Drost J, Mantovani F, Tocco F, Elkon R, Comel A, Holstege H, Kerkhoven R, Jonkers J, Voorhoeve PM, Agami R, et al. BRD7 is a candidate tumour suppressor gene required for p53 function. Nat Cell Biol. 2010; 12:380–389. [PubMed: 20228809]

Fonseca SG, Gromada J, Urano F. Endoplasmic reticulum stress and pancreatic beta-cell death. Trends Endocrinol Metab. 2011; 22:266–274. [PubMed: 21458293]

Guilherme A, Virbasius JV, Puri V, Czech MP. Adipocyte dysfunctions linking obesity to insulin resistance and type 2 diabetes. Nat Rev Mol Cell Biol. 2008; 9:367–377. [PubMed: 18401346]

Harte MT, O'Brien GJ, Ryan NM, Gorski JJ, Savage KI, Crawford NT, Mullan PB, Harkin DP. BRD7, a subunit of SWI/SNF complexes, binds directly to BRCA1 and regulates BRCA1-dependent transcription. Cancer Res. 2010; 70:2538–2547. [PubMed: 20215511]

Hevener AL, Febbraio MA. The 2009 stock conference report: inflammation, obesity and metabolic disease. Obes Rev. 2010; 11:635–644. [PubMed: 20002885]

Kadowaki T, Hara K, Yamauchi T, Terauchi Y, Tobe K, Nagai R. Molecular mechanism of insulin resistance and obesity. Exp Biol Med (Maywood). 2003; 228:1111–1117. [PubMed: 14610248]

Kaeser MD, Aslanian A, Dong MQ, Yates JR 3rd, Emerson BM. BRD7, a novel PBAF-specific SWI/SNF subunit, is required for target gene activation and repression in embryonic stem cells. J Biol Chem. 2008; 283:32254–32263. [PubMed: 18809673]

Kahn BB, Flier JS. Obesity and insulin resistance. J Clin Invest. 2000; 106:473–481. [PubMed: 10953022]

Kenyon CJ. The genetics of ageing. Nature. 2010; 464:504–512. [PubMed: 20336132]

Kitamura Y, Accili D. New insights into the integrated physiology of insulin action. Rev Endocr Metab Disord. 2004; 5:143–149. [PubMed: 15041790]

Konner AC, Bruning JC. Selective insulin and leptin resistance in metabolic disorders. Cell Metab. 2012; 16:144–152. [PubMed: 22883229]

Lee AH, Iwakoshi NN, Glimcher LH. XBP-1 regulates a subset of endoplasmic reticulum resident chaperone genes in the unfolded protein response. Mol Cell Biol. 2003; 23:7448–7459. [PubMed: 14559994]

Lee J, Sun C, Zhou Y, Gokalp D, Herrema H, Park SW, Davis RJ, Ozcan U. p38 MAPK-mediated regulation of Xbp1s is crucial for glucose homeostasis. Nat Med. 2011; 17:1251–1260. [PubMed: 21892182]

Lee K, Tirasophon W, Shen X, Michalak M, Prywes R, Okada T, Yoshida H, Mori K, Kaufman RJ. IRE1-mediated unconventional mRNA splicing and S2P-mediated ATF6 cleavage merge to

regulate XBP1 in signaling the unfolded protein response. Genes Dev. 2002; 16:452–466. [PubMed: 11850408]

Luo J, Field SJ, Lee JY, Engelman JA, Cantley LC. The p85 regulatory subunit of phosphoinositide 3-kinase down-regulates IRS-1 signaling via the formation of a sequestration complex. J Cell Biol. 2005; 170:455–464. [PubMed: 16043515]

Mantovani F, Drost J, Voorhoeve PM, Del Sal G, Agami R. Gene regulation and tumor suppression by the bromodomain-containing protein BRD7. Cell Cycle. 2010; 9:2777–2781. [PubMed: 20647772]

Marciniak SJ, Ron D. Endoplasmic reticulum stress signaling in disease. Physiol Rev. 2006; 86:1133–1149. [PubMed: 17015486]

Merksamer PI, Papa FR. The UPR and cell fate at a glance. J Cell Sci. 2010; 123:1003–1006. [PubMed: 20332117]

Muoio DM, Newgard CB. Obesity-related derangements in metabolic regulation. Annu Rev Biochem. 2006; 75:367–401. [PubMed: 16756496]

Nakatani Y, Kaneto H, Kawamori D, Yoshiuchi K, Hatazaki M, Matsuoka TA, Ozawa K, Ogawa S, Hori M, Yamasaki Y, et al. Involvement of endoplasmic reticulum stress in insulin resistance and diabetes. J Biol Chem. 2005; 280:847–851. [PubMed: 15509553]

Ozawa K, Miyazaki M, Matsuhisa M, Takano K, Nakatani Y, Hatazaki M, Tamatani T, Yamagata K, Miyagawa J, Kitao Y, et al. The endoplasmic reticulum chaperone improves insulin resistance in type 2 diabetes. Diabetes. 2005; 54:657–663. [PubMed: 15734840]

Ozcan L, Ergin AS, Lu A, Chung J, Sarkar S, Nie D, Myers MG Jr, Ozcan U. Endoplasmic reticulum stress plays a central role in development of leptin resistance. Cell Metab. 2009; 9:35–51. [PubMed: 19117545]

Ozcan U, Cao Q, Yilmaz E, Lee AH, Iwakoshi NN, Ozdelen E, Tuncman G, Gorgun C, Glimcher LH, Hotamisligil GS. Endoplasmic reticulum stress links obesity, insulin action, and type 2 diabetes. Science. 2004; 306:457–461. [PubMed: 15486293]

Ozcan U, Ozcan L, Yilmaz E, Duvel K, Sahin M, Manning BD, Hotamisligil GS. Loss of the tuberous sclerosis complex tumor suppressors triggers the unfolded protein response to regulate insulin signaling and apoptosis. Mol Cell. 2008; 29:541–551. [PubMed: 18342602]

Ozcan U, Yilmaz E, Ozcan L, Furuhashi M, Vaillancourt E, Smith RO, Gorgun CZ, Hotamisligil GS. Chemical chaperones reduce ER stress and restore glucose homeostasis in a mouse model of type 2 diabetes. Science. 2006; 313:1137–1140. [PubMed: 16931765]

Palade GE. The endoplasmic reticulum. J Biophys Biochem Cytol. 1956; 2:85–98. [PubMed: 13357527]

Park SW, Ozcan U. Potential for therapeutic manipulation of the UPR in disease. Semin Immunopathol. 2013; 35:351–373. [PubMed: 23572207]

Park SW, Zhou Y, Lee J, Lu A, Sun C, Chung J, Ueki K, Ozcan U. The regulatory subunits of PI3K, p85alpha and p85beta, interact with XBP-1 and increase its nuclear translocation. Nat Med. 2010a; 16:429–437. [PubMed: 20348926]

Park SW, Zhou Y, Lee J, Ozcan U. Sarco(endo)plasmic reticulum Ca2+-ATPase 2b is a major regulator of endoplasmic reticulum stress and glucose homeostasis in obesity. Proc Natl Acad Sci U S A. 2010b; 107:19320–19325. [PubMed: 20974941]

Peng C, Liu HY, Zhou M, Zhang LM, Li XL, Shen SR, Li GY. BRD7 suppresses the growth of Nasopharyngeal Carcinoma cells (HNE1) through negatively regulating beta-catenin and ERK pathways. Mol Cell Biochem. 2007; 303:141–149. [PubMed: 17458518]

Peng C, Zhou J, Liu HY, Zhou M, Wang LL, Zhang QH, Yang YX, Xiong W, Shen SR, Li XL, et al. The transcriptional regulation role of BRD7 by binding to acetylated histone through bromodomain. J Cell Biochem. 2006; 97:882–892. [PubMed: 16265664]

Qatanani M, Lazar MA. Mechanisms of obesity-associated insulin resistance: many choices on the menu. Genes Dev. 2007; 21:1443–1455. [PubMed: 17575046]

Ron D, Walter P. Signal integration in the endoplasmic reticulum unfolded protein response. Nat Rev Mol Cell Biol. 2007; 8:519–529. [PubMed: 17565364]

Russell SJ, Kahn CR. Endocrine regulation of ageing. Nat Rev Mol Cell Biol. 2007; 8:681–691. [PubMed: 17684529]

Schroder M, Kaufman RJ. The mammalian unfolded protein response. Annu Rev Biochem. 2005; 74:739–789. [PubMed: 15952902]

Sun B, Karin M. Obesity, inflammation, and liver cancer. J Hepatol. 2012; 56:704–713. [PubMed: 22120206]

Taguchi A, Wartschow LM, White MF. Brain IRS2 signaling coordinates life span and nutrient homeostasis. Science. 2007; 317:369–372. [PubMed: 17641201]

Ueki K, Fruman DA, Brachmann SM, Tseng YH, Cantley LC, Kahn CR. Molecular balance between the regulatory and catalytic subunits of phosphoinositide 3-kinase regulates cell signaling and survival. Mol Cell Biol. 2002; 22:965–977. [PubMed: 11784871]

Ueki K, Fruman DA, Yballe CM, Fasshauer M, Klein J, Asano T, Cantley LC, Kahn CR. Positive and negative roles of p85 alpha and p85 beta regulatory subunits of phosphoinositide 3-kinase in insulin signaling. J Biol Chem. 2003; 278:48453–48466. [PubMed: 14504291]

Walter P, Ron D. The unfolded protein response: from stress pathway to homeostatic regulation. Science. 2011; 334:1081–1086. [PubMed: 22116877]

Wang S, Kaufman RJ. The impact of the unfolded protein response on human disease. J Cell Biol. 2012; 197:857–867. [PubMed: 22733998]

Winnay JN, Boucher J, Mori MA, Ueki K, Kahn CR. A regulatory subunit of phosphoinositide 3-kinase increases the nuclear accumulation of X-box-binding protein-1 to modulate the unfolded protein response. Nat Med. 2010; 16:438–445. [PubMed: 20348923]

Winnay JN, Dirice E, Liew CW, Kulkarni RN, Kahn CR. p85alpha deficiency protects beta-cells from endoplasmic reticulum stress-induced apoptosis. Proc Natl Acad Sci U S A. 2014; 111:1192–1197. [PubMed: 24395790]

Yoshida H, Matsui T, Yamamoto A, Okada T, Mori K. XBP1 mRNA is induced by ATF6 and spliced by IRE1 in response to ER stress to produce a highly active transcription factor. Cell. 2001; 107:881–891. [PubMed: 11779464]

Zhang K, Kaufman RJ. From endoplasmic-reticulum stress to the inflammatory response. Nature. 2008; 454:455–462. [PubMed: 18650916]

Zhou J, Ma J, Zhang BC, Li XL, Shen SR, Zhu SG, Xiong W, Liu HY, Huang H, Zhou M, et al. BRD7, a novel bromodomain gene, inhibits G1-S progression by transcriptionally regulating some important molecules involved in ras/MEK/ERK and Rb/E2F pathways. J Cell Physiol. 2004; 200:89–98. [PubMed: 15137061]

Zhou Y, Lee J, Reno C, Sun C, Park S, Chung J, Lee J, Fisher S, White M, Biddinger S, et al. Regulation of glucose homeostasis through a XBP-1–FoxO1 interaction. Nature Medicine. 201110.1038/nm.2293

Highlights

- BRD7 interacts with p85α and p85β and increases their nuclear translocation.
- BRD7 increases the nuclear translocation of XBP1s in a p85-dependent manner.
- BRD7 levels are reduced in the liver of obese and diabetic mice.
- BRD7 re-establishes glucose homeostasis in obese and diabetic mice.

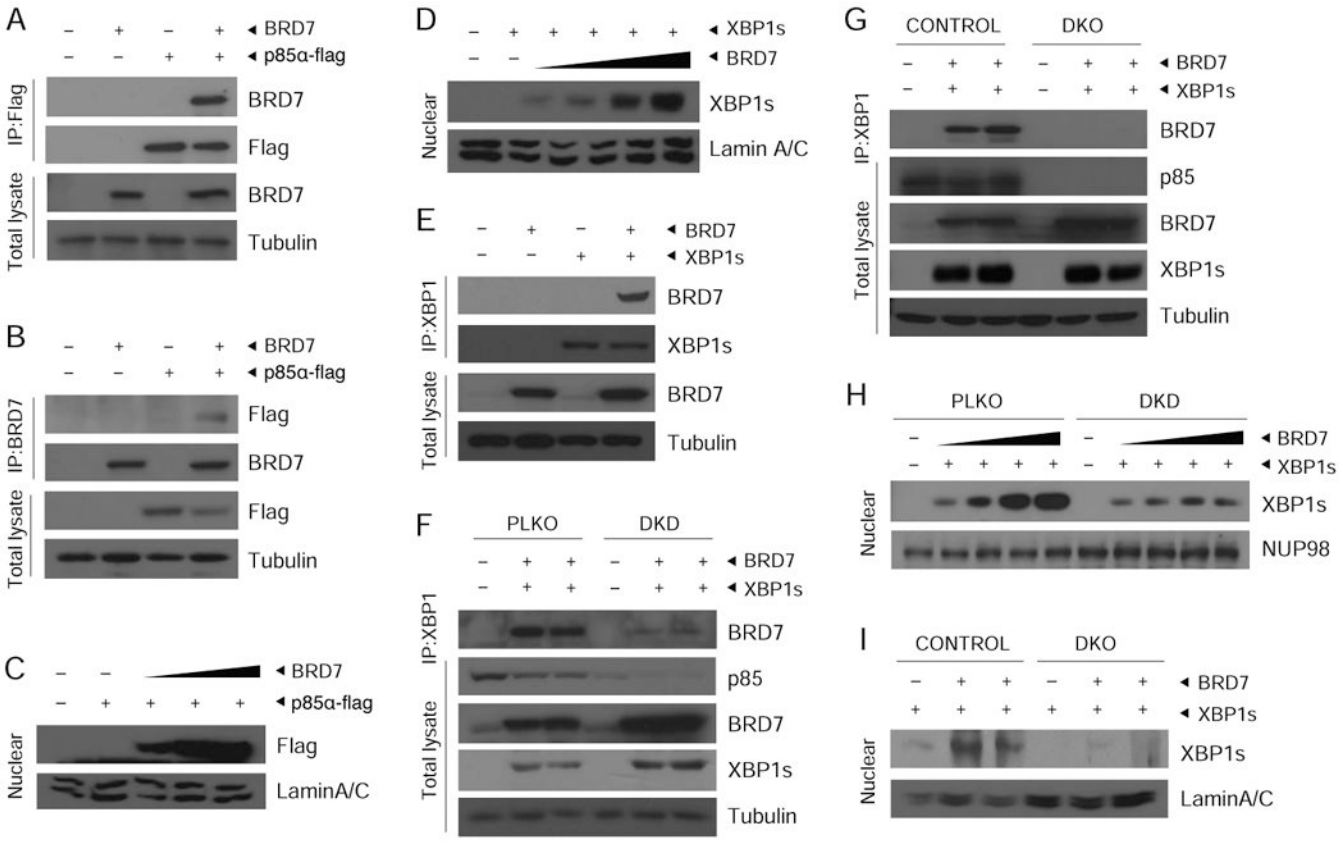

Figure 1. BRD7 binds to p85α and increases its nuclear translocation

(A) Immunoblotting for BRD7 and flag-tagged p85α proteins after immunoprecipitation of p85α from 293HEK cells that were infected with Ad-BRD7 alone; or Ad-p85α-flag alone; or Ad-BRD7 and Ad-p85α-flag. Total lysates were immunoblotted for BRD7 and tubulin. (B) Immunoblots of flag-p85α and BRD7 after BRD7 immunoprecipitation from 293HEK cells that were infected with the indicated adenoviruses. (C) Nuclear protein levels of p85α in 293HEK cells infected with increasing doses of Ad-BRD7 and a constant dose of Ad-p85α-flag. LaminA/C was used as a control for nuclear protein level. (D) Nuclear protein levels of XBP-1s in 293HEK cells infected with increasing doses of Ad-BRD7 and a constant dose of XBP1s. (E) Immunoblotting for BRD7 and XBP1s following immunoprecipitation with XBP1-specific antibody. Total protein levels of BRD7 and tubulin are shown below. (F) BRD7 immunoblotting after XBP1 immunoprecipitation from DKD (p85α and p85β double knock down) and PLKO (control) cells that were infected with Ad-BRD7 and Ad-XBP1s. Total protein amounts of p85s, BRD7, XBP1s, and tubulin are shown below. (G) Immunoblotting for BRD7 protein after XBP1 immunoprecipitation from DKO (p85α and p85β double knock out) and its control cells that were infected with Ad-BRD7 and Ad-XBP1s. Total protein amounts of p85s, BRD7, XBP1 and tubulin are shown below. (H) Nuclear protein amounts of XBP1s in PLKO and DKD cells infected with increasing doses of Ad-BRD7 and a constant dose of XBP1s. NUP98 was used as a control for nuclear protein level. (I) Western blot for XBP1s in PLKO and DKO cells infected with Ad-BRD7 and Ad-XBP1s. LaminA/C was used as a control. Each experiments was independently repeated three times.

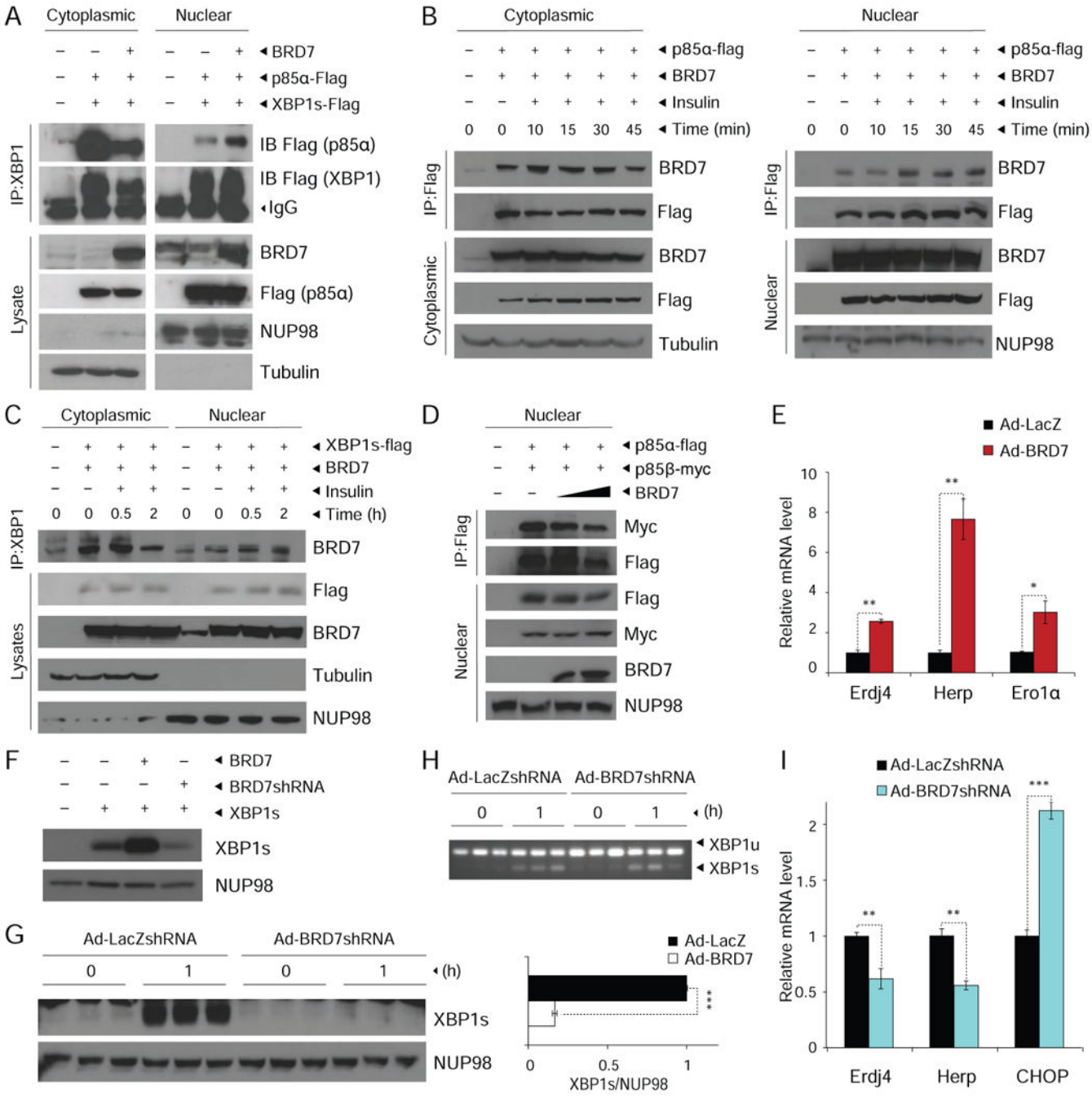

Figure 2. BRD7 increases the nuclear translocation of XBP1s

(A) Flag-p85α and flag-XBP1s immunoblots after XBP1 immunoprecipitation from cytoplasmic and nuclear protein fractions of 293HEK cells that were infected with Ad-p85α-flag and Ad-XBP1s-flag; or together with Ad-BRD7. Total lysates were immunoblotted for BRD7 and p85α. NUP98 and tubulin were used as a control for nuclear and cytoplasmic protein levels, respectively. (B) BRD7 and flag-p85α immunoblots after flag immunoprecipitation from cytoplasmic and nuclear protein fractions of 293HEK cells that were infected with Ad-p85α-flag and Ad-BRD7, followed by insulin treatment at 500

nM for indicated times. Each cytoplasmic and nuclear protein lysates was immunoblotted for BRD7, flag, and tubulin/or NUP98. (C) BRD7 immunoblotting in XBP1 immunoprecipitates after insulin (500 nM) stimulation. Protein lysates were immunoblotted for indicated antibodies. (D) Nuclear protein amounts of p85α and p85β in 293HEK cells infected with a constant dose of Ad-85α-flag and Ad-p85β-myc and increasing doses of Ad-BRD7. (E) Expression levels of XBP1 target genes, *Erdj4*, *Her*p, and *Ero1α* in MEFs infected with Ad-LacZ or Ad-BRD7. (F) Western blot analysis for nuclear XBP1s proteins in 293HEK cells that were infected with the indicated adenoviruses. (G-I) Eight-week-old male wild-type mice were injected with Ad-LacZshRNA or Ad-BRD7shRNA (1.5×10^8 pfu/g, n=6 for each group) through the tail vein. (G) Nuclear XBP1s protein amounts at 24 hours of fasting and during one hour of refeeding on day seven post-injection (left). NUP98 was used as a control. Quantification of the western blot showing the ratio of XBP1s to NUP98 (right). (H) XBP1 mRNA splicing assay in Ad-LacZshRNA or Ad-BRD7shRNA injected mice at 24 hours of fasting and one hour after refeeding. (I) Relative mRNA levels of *Erdj4*, *Herp*, and *CHOP* in the liver of Ad-LacZshRNA or Ad-BRD7shRNA injected mice after six hours of fasting. Error bars are represented as mean ± SEM., *P* values were determined by Student's *t*-test. **P*<0.05, ***P* <0.01, ****P* <0.001. Each experiments was independently repeated three times.

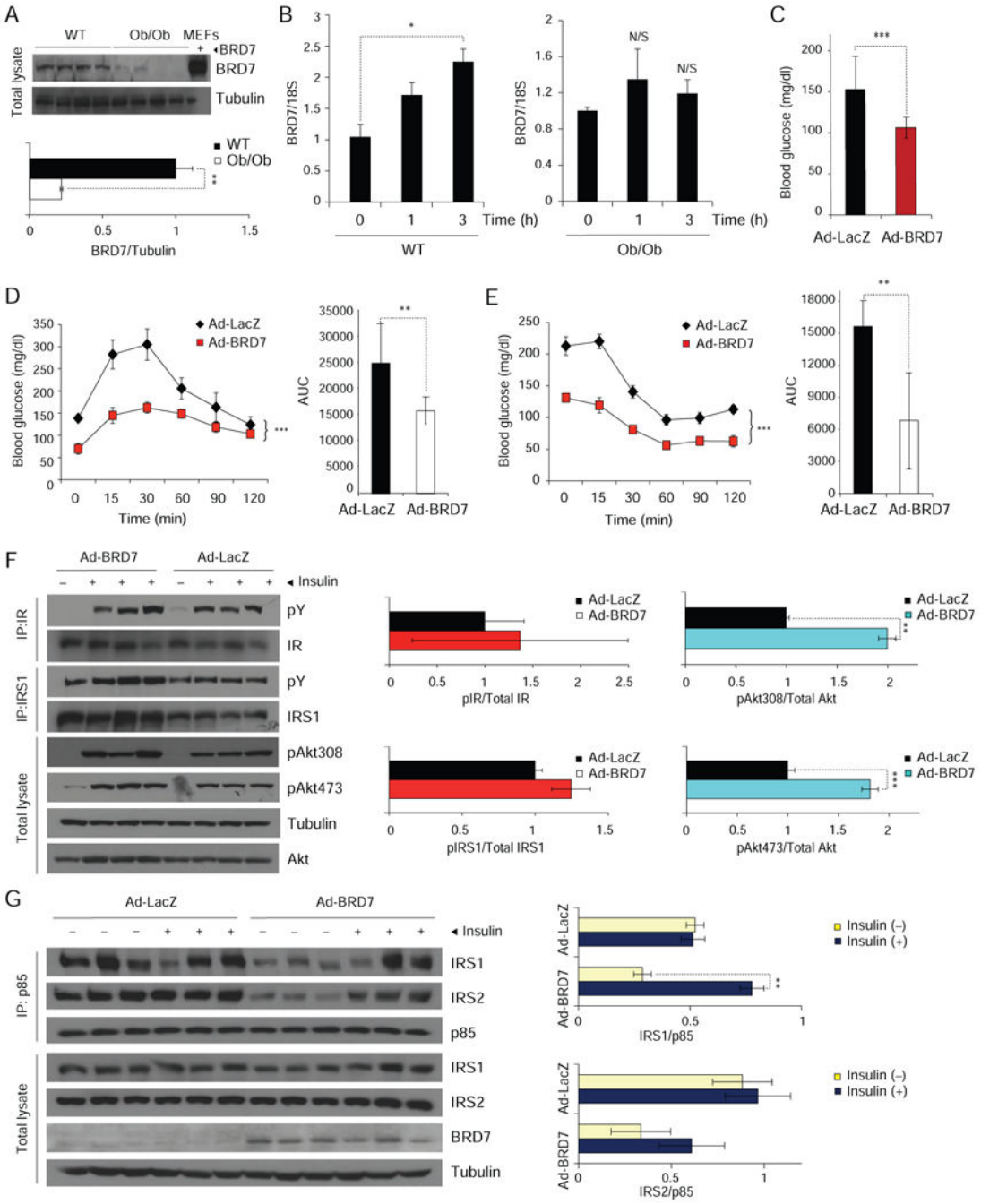

Figure 3. Restoration of BRD7 in the liver of the *ob/ob* mice improves glucose tolerance and establishes euglycemia

(A) Total BRD7 protein amounts in the liver of lean wild-type and *ob*/*ob* mice at six hours of fasting (top). Quantification of the western blot showing the ratio of BRD7 to tubulin (bottom). (B) BRD7 mRNA levels in the wild-type and *ob*/*ob* mice's livers during 24 hours of fasting and one and three hours of refeeding states. (C-G) Eight-week-old male *ob*/*ob* mice were injected with Ad-BRD7 or Ad-LacZ (1×10^8 pfu/g, n=6 for each group) as a control through the tail vein. (C) Blood glucose levels (mg/dl) after six hours fasting on day three of the injections. (D) Glucose tolerance test (GTT) on day five post-injection (left).

Area under the curve of GTT (right). (E) Insulin tolerance test (ITT) on day seven post-injection (left). Area under the curve of ITT (right). (F) *In vivo* insulin receptor signaling in the liver of Ad-LacZ or Ad-BRD7 injected *ob*/*ob* mice on day eight after injection (left). Quantifications of the western blots (right). (G) Immunoblots of IRS1, IRS2, and p85 after p85 immunoprecipitation of the liver tissues that were infused with insulin in Ad-LacZ and Ad-BRD7 injected *ob*/*ob* mice (left). Quantifications of the western blots (right). Error bars are represented as mean ± SEM., *P* values in (B) and (C) were determined by Student's *t*-test. Significance in (D) and (E) was determined by two-way ANOVA with Bonferroni multiple-comparison analysis. **P*<0.05, ***P* <0.01, ****P* <0.001. Experiments were repeated in three independent cohorts.

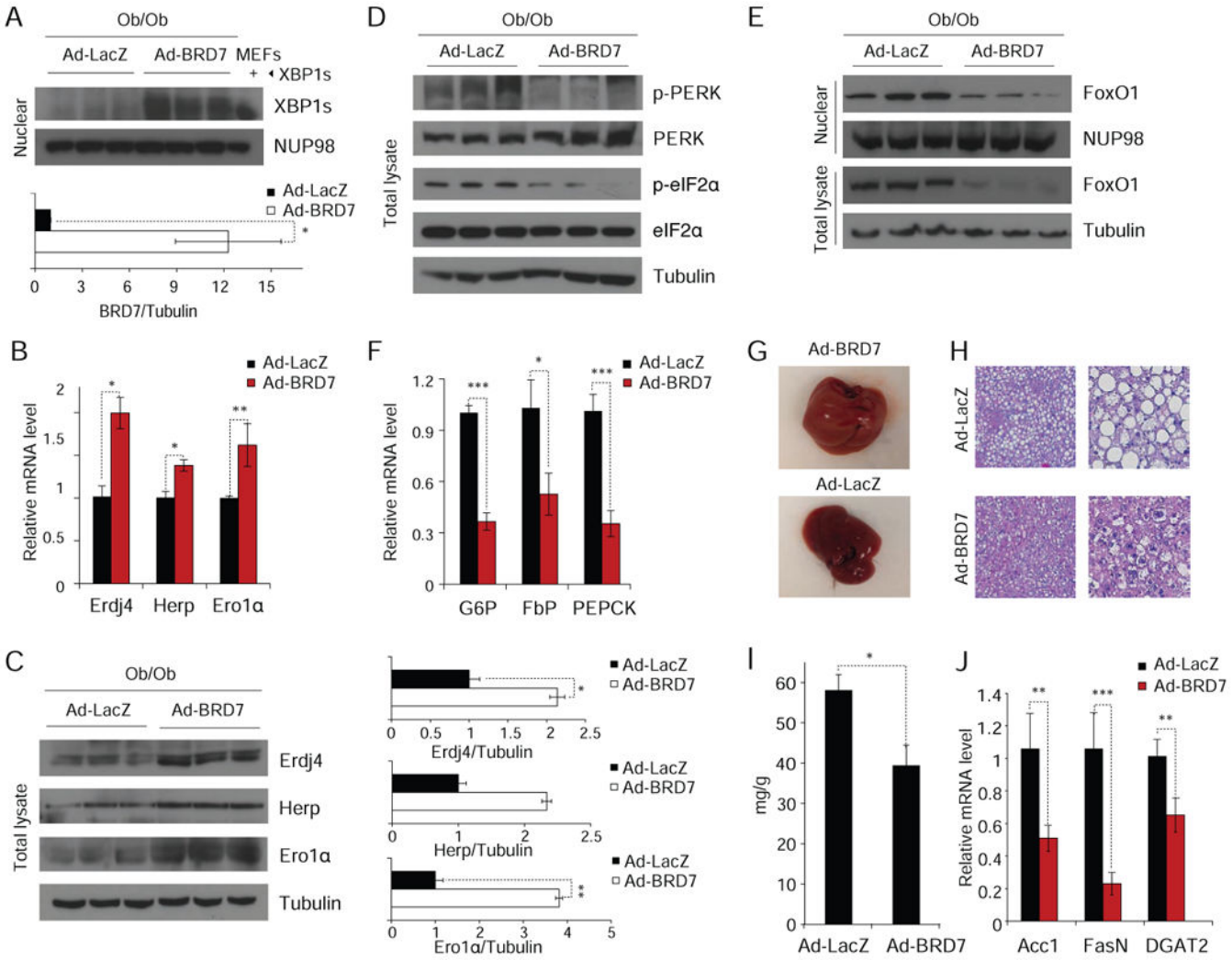

Figure 4. Restoration of BRD7 in the liver of the *ob/ob* mice releases ER stress and displays improved phenotypes

Eight-week-old male *ob/ob* mice were injected with Ad-BRD7 or Ad-LacZ (1×10^8 pfu/g, n=6 for each group) as a control through the tail vein. (A) Western blots for nuclear XBP1s protein on day eight post-injection (top). Quantification of the western blot showing the ratio of BRD7 to tubulin (bottom). (B-C) mRNA and protein levels of XBP1s target genes in the liver of Ad-LacZ and Ad-BRD7 injected mice after six hours of fasting were analyzed by qPCR (B) and western blot (C, left). Quantifications of the western blots (C, right). (D) PERK phosphorylation on Thr980, total PERK, eIF2α phosphorylation on Ser51, and total eIF2α protein levels in the liver of Ad-LacZ and Ad-BRD7 injected *ob*/*ob* mice were analyzed by western blot. (E) Total and nuclear amounts of FoxO1 protein in the liver of Ad-LacZ- or Ad-BRD7-injected *ob*/*ob* mice. (F) Relative mRNA levels of *G6p*, *Fb*p, and *Pepck*. (G) Macroscopic view of the liver of Ad-LacZ injected (top) and Ad-BRD7 injected (bottom) *ob*/*ob* mice. (H) H&E staining of liver sections in 4x (left) and 10x (right) magnifications. (I) Triglyceride contents (mg/g) in the liver. (J) Relative mRNA levels of *Acc1*, *FasN*, and *Dgat2*. Error bars are represented as mean ± SEM., P values were

determined by Student's t-test. (*p<0.05, **p<0.01, ***p<0.001). Experiments were repeated in three independent cohorts.

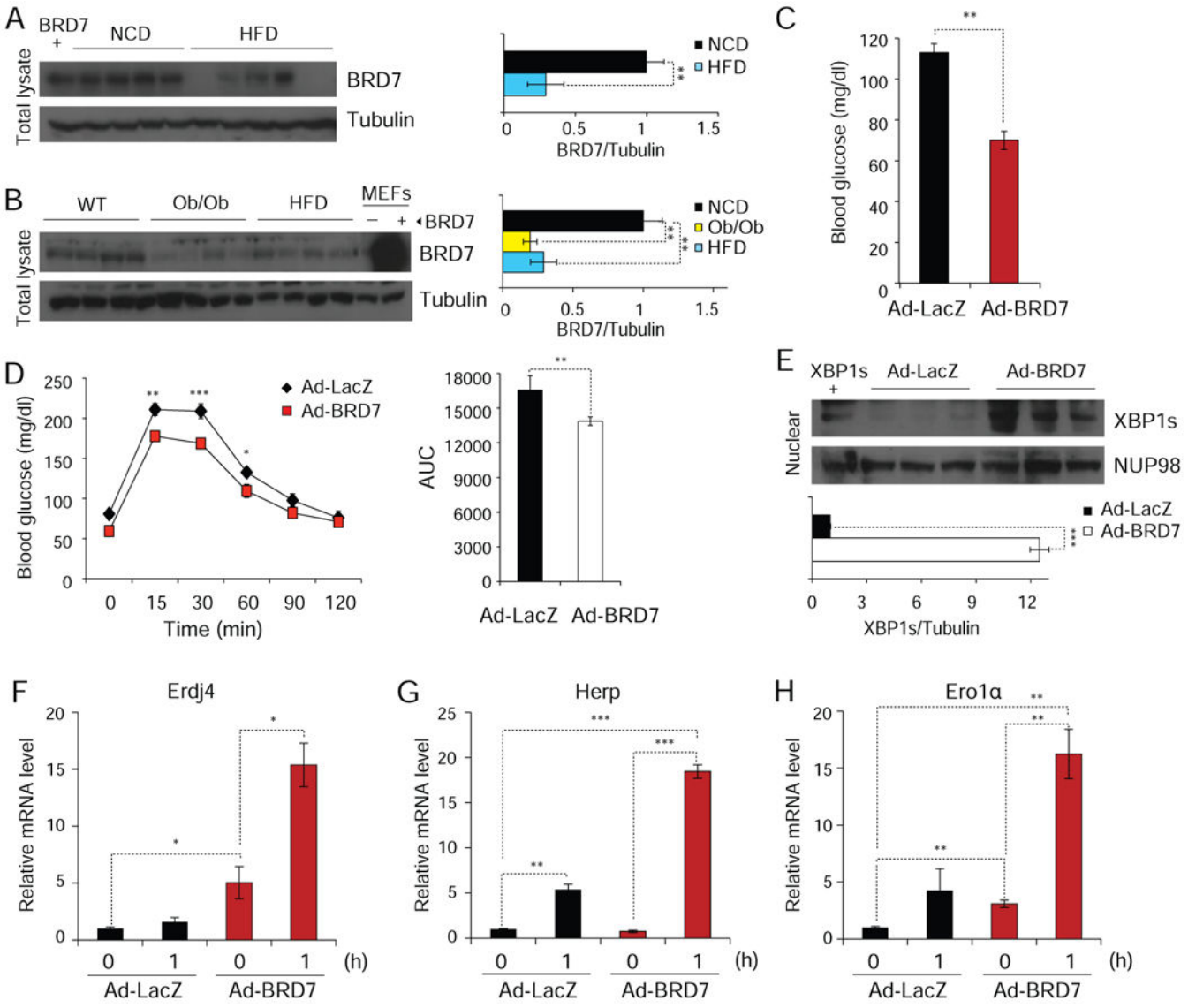

Figure 5. Restoration of BRD7 in the liver of the diet-induced obese (DIO) mice improves glucose tolerance and increases XBP1s nuclear translocation

(A) Total BRD7 protein amounts in the liver of lean wild-type that were fed either on normal chow diet (NCD) or high fat diet (HFD) at six hours of fasting (left). Quantification of the western blot showing the ratio of BRD7 to tubulin (right). (B) Western blot for BRD7 protein levels from the total lysates of wild-type (NCD), *ob*/*ob*, and HFD mice (left). Tubulin was used as a control. Quantification of the western blot showing the ratio of BRD7 to tubulin (right). (C-H) Mice that were fed either on NCD or HFD were injected with Ad-BRD7 or Ad-LacZ (5×10^7 pfu/g, n=6 for each group) through the tail vein. (C) The graph shows the blood glucose levels (mg/dl) after six hour fasting on day three of the injections. (D) Glucose tolerance test (GTT) on post-injection day five post-injection (left). Area under the curve of GTT (right). (E) XBP1s nuclear protein amounts in the liver lysates (top). Quantification of the western blot showing the ratio of XBP1s to tubulin (bottom). (F-H) Mice were fasted for 24 hours and refed for 0 and 1 hour. Relative mRNA levels of *Erdj4*,

Herp, and *Ero1α* were determined by qPCR. Error bars are represented as mean ± SEM., *P* values in (A-C and E-H) were determined by Student's *t*-test. Significance in (D) was determined by two-way ANOVA with Bonferroni multiple-comparison analysis. **P*<0.05, ***P* <0.01, ****P* <0.001. Experiments were repeated in three independent cohorts.